# PERFORMANCE IMPROVEMENT FOR THE SINGLE CARRIER IN FBMC SYSTEMS BY PAPR REDUCTION

Mohammed A. Salem[1], Mohamed A. Aboul-Dahab[2],
Sherine M. Abd El-kader[3] and Radwa A. Roshdy[1]

[1]Department of Electrical Engineering, Higher Technological Institute,
Tenth of Ramadan city, Egypt
[2]Department of Electronics and Communications Engineering, Arab Academy for
Science & Technology and Maritime Transport, Cairo, Egypt
[3]Department of Computers and Systems, Electronics Research Institute, Giza, Egypt

***ABSTRACT***

*The benefits of Filter Bank Multicarrier (FBMC) make it an attractive waveform instead of orthogonal frequency division multiplexing (OFDM). However, a high peak-to-average power ratio (PAPR) is a significant drawback in FBMC. Exploiting a single carrier effect is considered an effective technique to reduce PAPR in FBMC systems with a small amount of additional complexity. Nevertheless, the PAPR reduction amount is different from the single carrier effect in the single carrier frequency division multiple access (SC-FDMA). This is because of the overlapping structure of the in-phase and quadrature (IQ) between offset quadrature amplitude modulation (OQAM) FBMC symbols. So, we introduce an algorithm, based on signal distortion techniques, to improve the performance of the single carrier effect techniques in the PAPR reduction for the FBMC systems. Simulation results depict that the single carrier effect techniques with the proposed algorithm achieve an extra amount of PAPR reduction compared to the same techniques without using the proposed algorithm. In addition, the simulation results show that the proposed algorithm maximizes the PAPR reduction amount without affecting the complexity.*

***KEYWORDS***

*Filter bank multicarrier, FBMC, DFT spreading, single carrier effect, generalized DFT, PAPR reduction.*

## 1. INTRODUCTION

Waveform design is considered the main entrance to 5G to increase data rates and the network capacity to get more services with a higher quality of services [1]-[3]. Orthogonal frequency division multiplexing (OFDM) has merits that do not exist in the previous waveforms; it has low complexity implementation as it is using FFT and IFFT, it has higher flexibility in maintaining adaptive modulation per subcarrier, it is also equalized simply and supports multiple input multiple outputs (MIMO) [4]-[5].

Although privileged by the previously mentioned merits, OFDM has several limitations that make it less efficient to achieve 5G requirements. It requires high synchronization accuracy, and any synchronization error leads to a detriment in the orthogonality and causes interference. It includes a cyclic prefix (CP) to prevent inter-symbol interference (ISI), which results in limiting the spectral efficiency. OFDM has round trip time (RTT) which makes it not very efficient in terms of communication signaling overhead to support M2M applications. In addition, OFDM has also high out-of-band emission, OOB, due to the large power side lobe [6]. So new waveforms are needed to replace the OFDM. FBMC is a strong candidate as a waveform-based

technique for 5G as an alternative to OFDM [7]-[9]. FBMC has various advantageous characteristics that make it a promising 5G waveform candidate. It does not include CP, and this increases bandwidth efficiency [10]. It also has more flexibility to manage the bandwidth of each sub-carrier and the degree of overlap because of using non-orthogonal carriers and it is more flexible to exploit cognitive radio white spaces [11]. In addition, FBMC has the lowest OOB compared to other 5G waveform candidates like universal filter multicarrier (UFMC), generalized frequency division multiplexing (GFDM), and filtered OFDM (F-OFDM). Moreover, FBMC also is more immune to frequency misalignment and synchronization errors [12]. Despite the previously mentioned merits of FBMC, it suffers from elevated levels of Peak to Average Power Ratio (PAPR) as it is a multicarrier modulation technique. High PAPR leads to a signal clipping at the receiver because of the high-power amplifier (HPA) nonlinearity region [13]. Consequently, effective suppression of the OOB emission of FBMC remains under consideration. Signal distortion techniques such as clipping and filtering, companding, and peak cancellation were used to reduce PAPR in multicarrier communication systems like OFDM, and FBMC by distorting the output of the synthesis filter bank before it passes through the HPA. However, using such techniques degrade the bit error rate (BER) performance of the system and this requires side information to be transmitted (SI). On the other hand, these SI result in exceeding the required bandwidth required for the transmission.

The Single carrier effect is considered a promising technique to reduce PAPR effectively in 4G uplink transmission, this technique is called single carrier frequency division multiple access (SC-FDMA). But using a single carrier effect technique in FBMC is not as good as in SC-FDMA. This is because of the staggering between in-phase and quadrature (IQ) channels utilizing various pulse-shaped structures for offset quadrature amplitude modulation (OQAM) [14]-[16].

### 1.1. Motivation and Contributions

The use of DFT spreading, DFT spreading with ITSM and GDFT, in FBMC systems causes a quite notable reduction of PAPR amount. The way to maximize the PAPR reduction amount is attained by increasing computational complexity and using SI. The alternative method to avoid using SI and at the same time reduce the BER degradation is to minimize the signal distortion amount is low as possible. So, we propose an algorithm based on signal distortion techniques for keeping the computational complexity unchanged while improving the Performance of the PAPR reduction in FBMC for the single carrier effect techniques without any need for SI overhead.

The main contributions in this paper are summarized as follows:

- The algorithm to improve the performance of the single carrier effect as a PAPR improvement technique for the FBMC is proposed without any complexity and SI overhead.
- The proposed technique is applied to other algorithms of the FBMC single carrier effect which are available in the literature [19]-[21].
- The PAPR performance of the single carrier effect techniques with the proposed algorithm is investigated at different numbers of subcarriers. From the simulation results, the proposed algorithm enables the other techniques of the single carrier effect to reduce PAPR more than SC-FDMA.

The rest of the paper is organized as follows: Section 2 introduces a literature review about the FBMC DFT spreading techniques for PAPR reduction. Section 3 reviews the structure of the FBMC system and other FBMC single carrier techniques that are available in the literature. In section 4 the proposed algorithm, to improve the single carrier affect performance is introduced.

In section 5 the simulation results are introduced. In section 6 the computational complexity of the single carrier techniques utilizing the proposed algorithm are compared to other conventional single-carrier techniques. Section 7 concludes the paper.

## 2. LITERATURE REVIEW

The discrete Fourier transform (DFT) spreading technique is one of the single carrier effect techniques and it is the technique that is used in SC-FDMA. In [17]-[19] the DFT spreading technique being used in FBMC for PAPR improvement but the amount of reduction of PAPR is far away from the PAPR improvement amount that is attained by SC-FDMA. This is due to in [17]-[19] the DFT spreading is applied directly to the FBMC system without taking the staggering between in-phase and quadrature (IQ) channels into consideration. In [20] the DFT spreading technique had been used in the case of Identically-time shifted modulation (ITSM). This condition is based on the phase shift pattern of the in-phase and quadrature channels. Although the DFT spreading with the ITSM condition makes use of the single carrier effect, the amount of PAPR reduction is not so significant. So, the authors in [20] proposed an ITSM algorithm to increase the PAPR reduction amount by producing four waveforms with different PAPR, and the one with minimum PAPR was chosen to be sent. But, using the ITSM algorithm caused more computational complexity and side information (SI). In [21], GDFT had been proposed in FBMC as a single carrier effect technique instead of DFT as the latter resulted in a marginal PAPR reduction. Although using GDFT spreading improves the PAPR reduction performance more than that of various single carrier techniques, the PAPR reduction amount is not still as good as SC-FDMA. So, the authors in [21] introduced an improvement algorithm to allow the GDFT spreading to enhance PAPR as efficiently as SC-FDMA. However, the computational complexity is increased but still better than the ITSM algorithm. In [22], a DFT is used as a precoding method in FBMC to modify the format of data transmission in a way such that the PAPR is reduced. In [23], The combination of pruned DFT with spread techniques removes IFFT effects and the PAPR can be reduced. In [24], the PAPR is reduced by using a hybrid system of STM and DFT single carrier technique at the expense of adding complexity overhead.

## 3. FBMC SINGLE CARRIER TECHNIQUES

Assume M subcarriers and N symbols; as shown in figure 1, the nth complex input symbol at $m^{th}$ subcarrier $x_{m,n}$ is represented by in-phase and quadrature components indicated by $d_{m,n}$ and $u_{m,n}$ respectively as shown below:

$$x_{m,n} = d_{m,n} + ju_{m,n} \tag{1}$$

The IQ input components $d_{m,n}$ is then multiplied by the phase shift patterns $\rho_{m,n}$ and $\sigma_{m,n}$ at each $m^{th}$ subcarrier of the upper and lower IFFT, respectively.

Although there are different patterns for the IQ phase shifts in literature [25]-[26], all these patterns must attain the next state:

$$\rho_{m,n} = \begin{cases} 1(or-1) & m = even \\ j(or-j) & n = odd \end{cases}$$
$$\sigma_{m,n} = \begin{cases} j(or-j) & m = even \\ 1(or-1) & n = odd \end{cases} \tag{2}$$

A prototype real symmetric filter with response $g_{m,n}(t)$ is used for filtering each subcarrier. This prototype filter is described by overlapping factor K, which is defined by the ratio of the duration of the filter impulse response to the symbol period T of each multicarrier. prototype filter with the overlapping factor participates effectively in suppressing symbol interference (ISI). Frequency spreading by the overlapping factor (K) is essential to implement the FBMC system, but this resulted in increasing system complexity; so, the polyphase network FFT (PPN-FFT) is used. Although it does not require frequency spreading this results in some additional processing [27]. A concise and simple explanation of PPN-FFT operation is given in [20]. Finally, the IQ components are shifted in time by half of the complex data symbol duration for each subcarrier T. this is done by applying the lower PPN output to the delay block T/2[27].

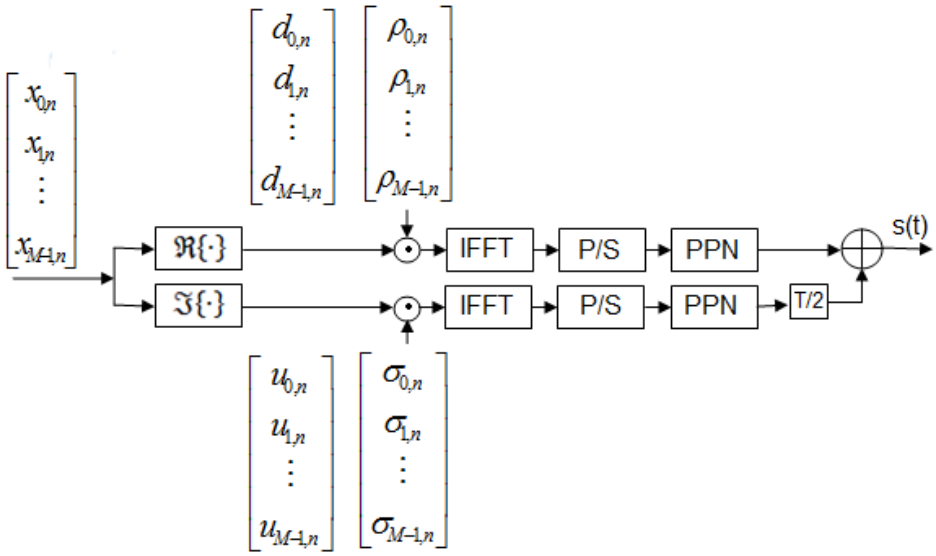


Figure 1. FBMC structure ⊙ represents the multiplication of element by element [21]

The transmitted signal based on the FBMC implementation that is shown in Fig. 1 is given by:

$$s(t) = \sum_{m=0}^{M-1} \sum_{n=0}^{N-1} x_{m,n} g(t-nT) e^{j\phi_{m,n}} e^{j\frac{2\pi mt}{T}} \tag{3}$$

where $x_{m,n}$ the complex FBMC input nth symbol is expressed in (1) and $g(t-nT)$ is a response of the prototype filter. Its length (l) is defined by {KN} where N represents the OQAM symbol numbers each subcarrier. $e^{j\phi_{m,n}}$ is the phase shift pattern where $\phi_{m,n} = \phi_o + \frac{\pi}{2}(m+n) \bmod \pi$, $e^{j\phi_{m,n}}$ is denoted by $\rho_{m,n}$ for real input symbols and is denoted by $\sigma_{m,n}$ for complex input symbols.

### 3.1. FBMC DFT spreading technique

In [17]-[19], the DFT spreading is applied directly to FBMC as the same as in the SC-FDMA system. This is depicted in figure 2. The input data symbol is applied to a DFT. their outputs are fed to the FBMC input.

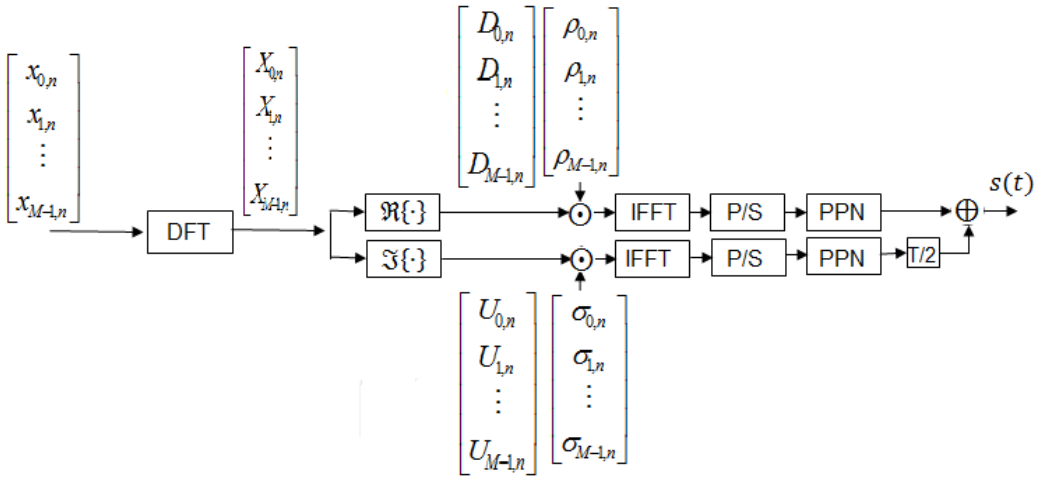


Figure 2. FBMC DFT spreading

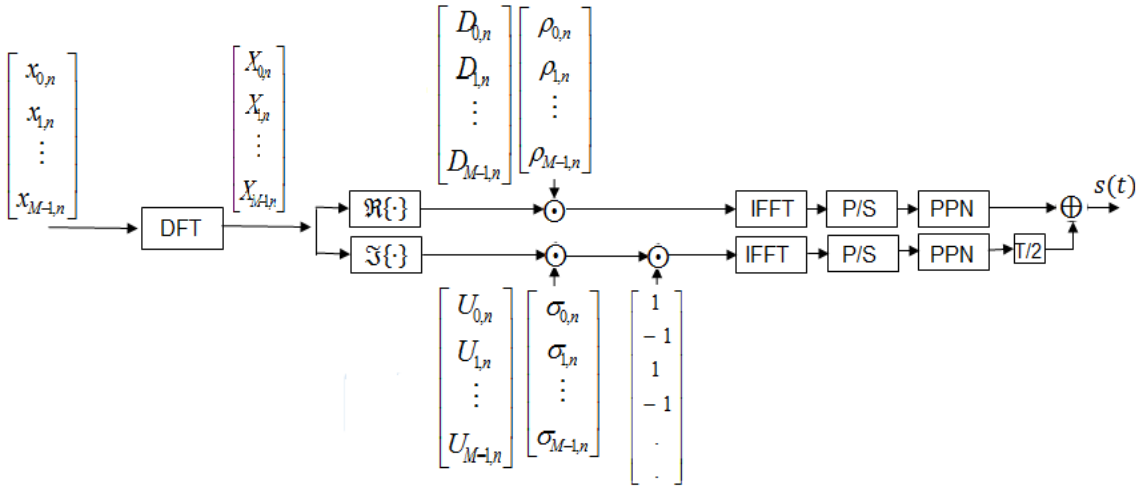


Figure 3. FBMC structure with ITSM spreading

## 3.2. ITSM Technique

In [20] single carrier property had been fully exploited by applying a condition of an identically time-shifted multicarrier (ITSM) to the DFT spreading. The ITSM condition is based on multiplying the phase shift pattern of the quadrature channel $\{\sigma_{m,n}\}$ by the term $(-1)^m$ , this is cleared in figure 3. Consequently, the multicarrier for the IQ channel appears identically time-shifted. However, the PAPR reduction amount was not so significant due to the overlapping interval among the OQAM symbols of IQ channels; the resultant reduction amount of the PAPR ranged from 0.6 dB to 0.8 dB.

## 3.3. FBMC with GDFT Spreading Technique

In GDFT spreading technique the complex input symbol was separated into in-phase and quadrature-phase terms before being applied to the GDFT as it is depicted in figure 4. Also, the phase shaping function was set to zero and mM/*2* in the case of the in-phase $\{d_{k,n}\}$ and quadrature

$\{u_{k,n}\}$ channel symbols, respectively. This indicates that the GDFT spreading technique is with a linear phase [21].

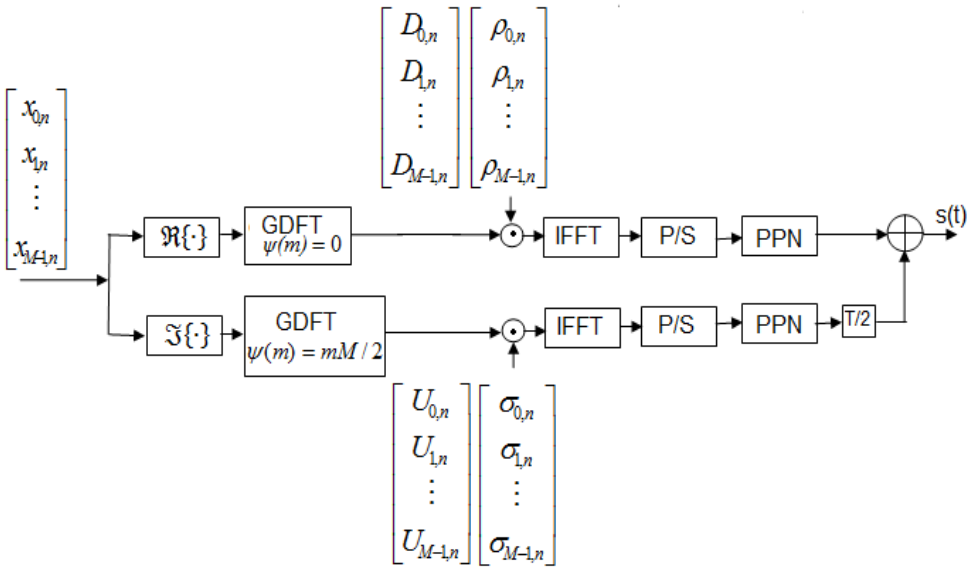


Figure 4. FBMC structure with GDFT spreading

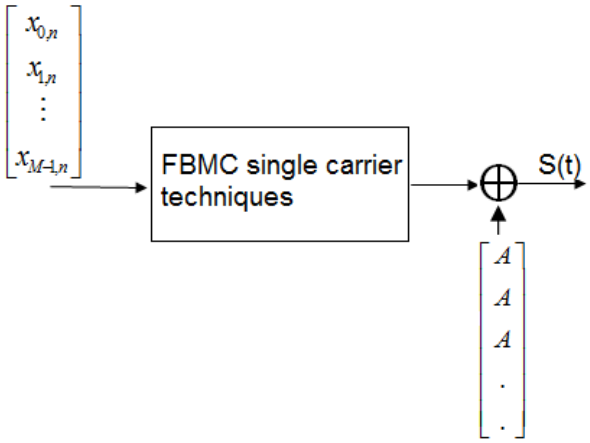


Figure 5. The improved FBMC single carrier structure

## 4. THE PROPOSED ALGORITHM

The PAPR of FBMC transmitted signal is defined as follows:

$$PAPR = \frac{\max\limits_{(n-1)T \le t \le nT} |s(t)|^2}{E\left[|s(t)|^2\right]} \quad n = 0,1,\ldots., \quad N-1 \tag{4}$$

where $\{\max |s(t)^2|\}$ and $\{E[|s(t)|^2]\}$ are the peak power and the average power of the transmitted signal, respectively and N is the number of transmitted symbols. To reduce the level of PAPR either reduce the Peak power or increase the average power. Reducing the Peak power was achieved in

signal distortion techniques such as clipping and peak signal cancellation techniques. In this method, the FBMC transmitted signal was clipped to a predefined value and as a result, PAPR is decreased. Nevertheless, clipping noise is a big problem at the receiver. To compensate for this noise, the receiver complexity was increased. If this noise wasn't compensated the signal BER performance will be degraded [28].

Increasing the average power is an alternative solution to reduce PAPR. This is done by increasing each FBMC symbol by a predetermined value (A). Although this will help in increasing the peak power the average power also increased and the final ratio will be decreased. At the receiver, each symbol will be decreased by a predetermined value added to it at the transmitter. Thus, there is no chance to exist something like noise clipping and the signal BER performance will not be affected. The block diagram of the single carrier techniques utilizing the improved algorithm is shown in figure 5.

The following steps illustrate the proposed algorithm for PAPR reduction as follows:

***Step 1:*** The input data frame to the FBMC system is at first divided into a consecutive number of symbol blocks equal to *W* and the number of symbols per each block equals to $\ell$.

***Step 2:*** The symbol index (n) is limited to the $(\ell th)$ data symbols block such that $0 \le n \le \ell W - 1$. So, the FBMC complex transmitted signal in (3) can be defined as where *M* is the number of subcarriers and $x_{m,n}$ is the complex FBMC input data:

$$s(t)_{\ell} = \sum_{m=0}^{M-1} \sum_{n=0}^{\ell W-1} x_{m,n} g(t-nT) e^{j\frac{2\pi mt}{T}} e^{j\phi_{m,n}} \tag{5}$$

**Step 3**: the amplitude of each FBMC symbol is increased by a predetermined small value A. thus (5) will be expressed as:

$$s(t) = \sum_{m=0}^{M-1} \sum_{n=0}^{\ell W-1} (x_{m,n} + A) g(t-nT) e^{j\phi_{m,n}} e^{j\frac{2\pi mt}{T}} \tag{6}$$

**Step 4**: The PAPR of each FBMC symbol is determined as follows:

$$PAPR = \frac{\max\limits_{(n-1)T \le t \le nT} (x_{m,n} + A)^2}{\sum\limits_{n=0}^{N} (x_{m,n} + A)^2 / N} \quad n = 1,\ldots,\ N-1 \tag{7}$$

**Step 5**: the PAPR of each block is calculated as the addition of the PAPR of each symbol as follows:

$$\text{PAPR}\big|_{\text{W}} = \sum_{n=0}^{\ell-1} \text{PAPR}\big|_{\ell} \tag{8}$$

**Algorithm 1**: the proposed algorithm

**Initialization**

W=16

$\ell$ =1

A=0.05

**Process**
**FOR** i=0: $W / \ell$
**FOR** ii=1: $\ell$
Calculate $s_{ii}(t)$ in equation (5)
**WHILE (**absolute value of $s_{ii}(t)$ > 0)
**DO**
Calculate $s_{ii}(t)$ in equation (6)
**END**

$$\text{PAPR(ii)}=\frac{\max\{|s_{ii}(t)|^2\}}{average\{|s_{ii}(t)|^2\}}$$

**END**
Calculate the PAPR in equation (8)
**END**
Calculate the PAPR in equation (9)

Finally, the total PAPR for the transmitted signal is calculated by the addition of the PAPR of each block as follows:

$$\text{PAPR}|_{\text{total}} = \sum_{n=0}^{W-1} \text{PAPR}|_{W} \tag{9}$$

The proposed algorithm is illustrated in algorithm 1.

## 5. SIMULATION RESULTS

### 5.1. PAPR Comparison

In this section, the PAPR performance of the single carrier techniques utilizing the proposed algorithm versus the conventional single-carrier techniques is discussed. Also, the transmitted FBMC and SC-OFDMA signals are included to be taken as a reference. Simulation results are performed through upgrading related m-file using MATLAB package version 2021a. The parameters on which the simulation is based are listed in Table 1. The simulation parameters are selected to be the same as the parameters that existed in [20] and [21] so that the obtained simulation results are fairly compared to other conventional single-carrier techniques in [20] and [21]. The PAPR performance is assessed by the complementary cumulative distribution function (CCDF) which is denoted by (PAPR0) [29-30]. The DFT spreading technique after using the proposed algorithm will be called the improved DFT, improved ITSM and improved GDFT.

Table 1. Simulation Parameters.

| **Parameter** | **VALUE** |
|---|---|
| FBMC FFT/IFFT size | 64, 128 |
| Subcarriers (M) numbers | 64,128 |
| Symbols/subcarriers numbers | 16 |
| Modulation | OQPSK |
| Type of prototype filter | PHYDYAS filter |
| Overlap factor | 4 |

It is observable from Fig. 6 that with a reference value of the CCDF equals $10^{-3}$, the single carrier techniques utilizing the proposed algorithm, namely improved DFT, improved ITSM and improved GDFT, enhances the PAPR amount over the conventional single-carrier techniques namely DFT, ITSM and GDFT by 3.4 dB, 3 dB and 2.6 dB, respectively. Compared to SC-OFDMA the single carrier techniques with the proposed algorithm increase the PAPR reduction amount by 1.2 dB, 1.3 dB and 1.9dB in case of improved DFT, improved ITSM and improved GDFT, respectively.

More PAPR performance improvements are achieved with the increase of subcarrier numbers as it is depicted in Fig.7. This is because in general the increasing of subcarrier numbers of results in increasing the PAPR amount and this is happening in the case of conventional single-carrier techniques. However, increasing the average power as in the proposed algorithm helps in reducing the amount of PAPR growth with the increase of subcarrier numbers. Consequently, the improved DFT, improved ITSM, and improved GDFT enhance the PAPR amount over DFT, ITSM and GDFT spreading by 3.7 dB, 3.2 dB, and 2.8 dB, respectively.

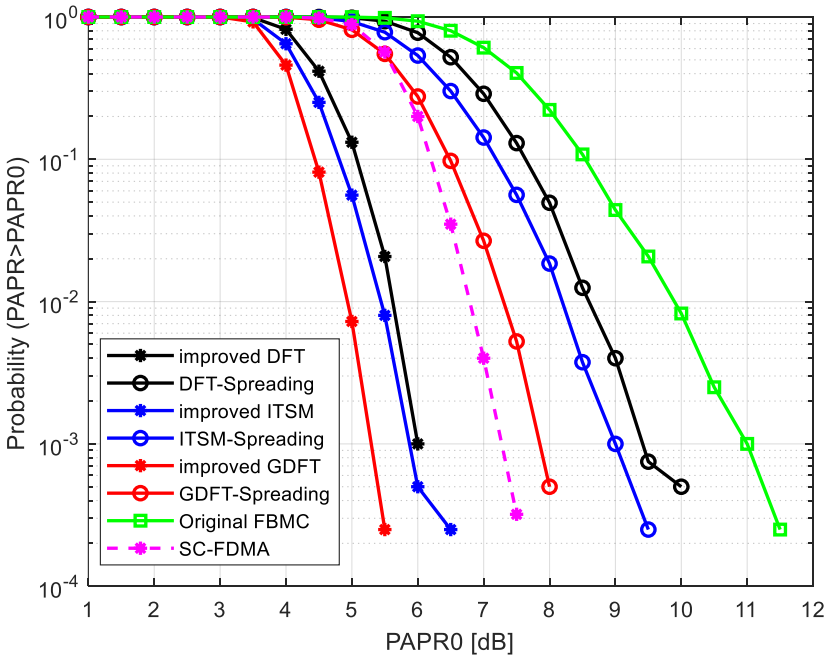


Figure 6. CCDFs comparison of the PAPR for the improved single carrier techniques for M=64.

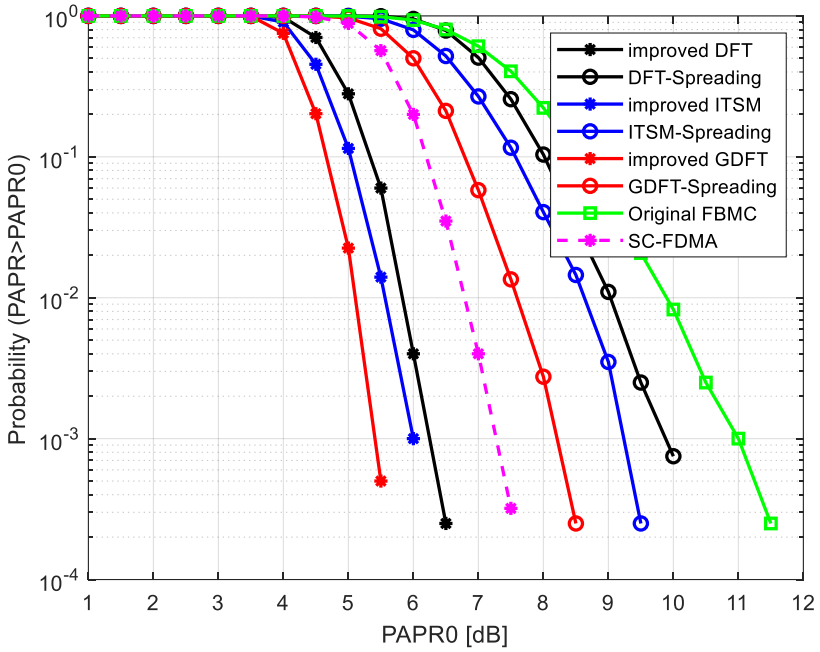


Figure 7. CCDFs comparison of the PAPR for the improved single carrier techniques for M=128.

### 5.2. PSD Comparison

The PSD characteristics for the FBMC single carrier techniques with and without using the improved algorithm are demonstrated in figure 8. Using a 0.2 normalized frequency as a mask, the DFT spreading and the GDFT technique before using the improved algorithm have lower OOB by -2 dB and -1 dB respectively compared to the same techniques after using the improved algorithm as it is shown in figure 8(a) and (c). In case of ITSM technique, the use of the improved algorithm does not affect the PSD performance as shown in figure 8(b).

## 6. COMPUTATIONAL COMPLEXITY COMPARISON

In this section, we introduce a computational complexity comparison of the single carrier techniques which utilize the proposed algorithm versus the conventional single-carrier techniques. The computational complexity is measured based on the number of additions and the real multiplication. However, measuring computational complexity based on the number of additions is not considered as multiplication carries the highest computational load. It is depicted in from Table 2 that the improved single carrier techniques have the same complexity overhead as that of the conventional techniques.

This is because the improved techniques are based on a proposed algorithm in which the amplitude of each FBMC symbol is increased by a predetermined value. Consequently, these additions do not have an impact on increasing the complexity overhead. With M subcarriers of power 2, the GDFT computational complexity is measured by 4x(M log2M), where the number (4) denotes the RMs number for one complex multiplication [31]. The M-point IFFT and DFT with M subcarriers of power 2 computational complexity are calculated by 4x(M log2M+2M) [32], and 4x(M/2)log2M respectively [33]. The PPN RMs number is given by 8KM [34].

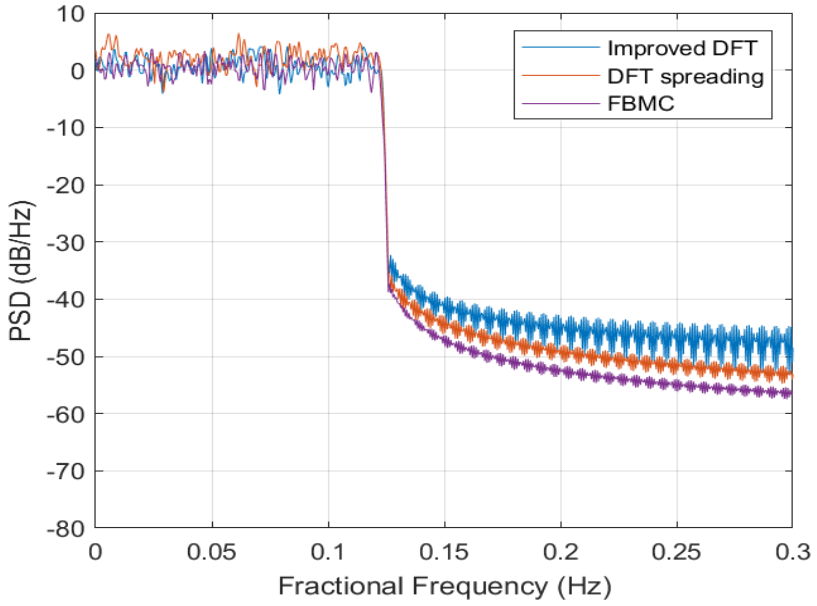
Improved DFT
DFT spreading
FBMC
PSD (dB/Hz)
Fractional Frequency (Hz)
10
0
-10
-20
-30
-40
-50
-60
-70
-80
0
0.05
0.1
0.15
0.2
0.25
0.3

(a)

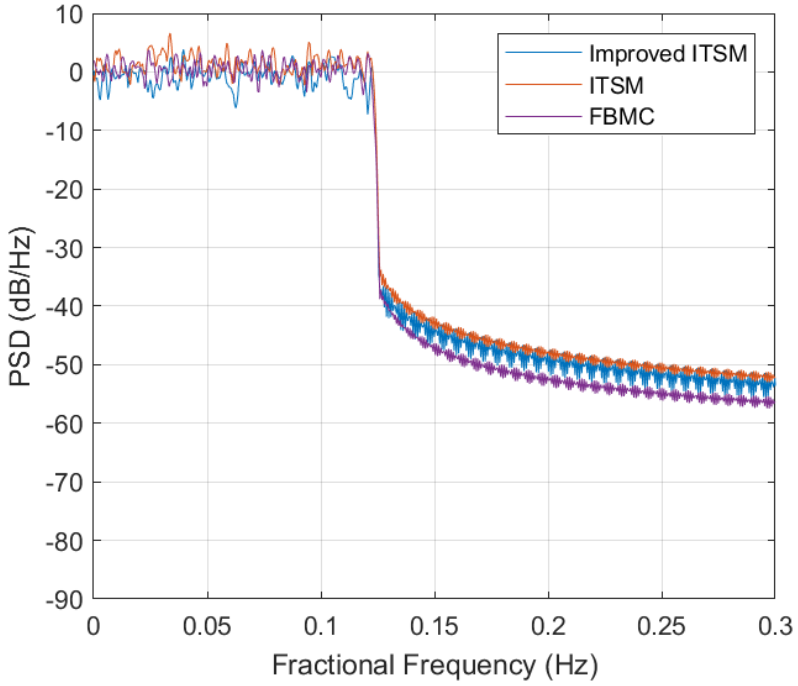
Improved ITSM
ITSM
FBMC
PSD (dB/Hz)
Fractional Frequency (Hz)
10
0
-10
-20
-30
-40
-50
-60
-70
-80
-90
0
0.05
0.1
0.15
0.2
0.25
0.3

(b)

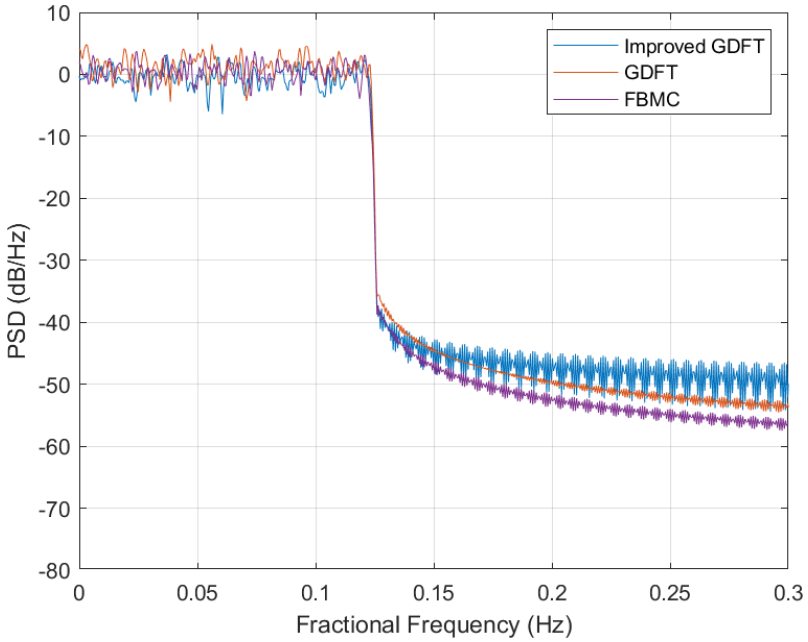


(c)

Figure 8. PSD characteristics for single carrier techniques with and without using the improved algorithm (a)DFT Spreading, (b) ITSM technique, and (c) GDFT spreading.

Table 2. Computational complexity comparison for different improved single carrier techniques.

| **Single carrier Technique** | **Main calculations** | **the Real Multiplication (RM) formula** | **Computational complexity/symbol period for M=64** | **Computational complexity/symbol period for M=128** |
|---|---|---|---|---|
| Original FBMC | 2 IFFTs and 2 PPNs | IFFT: $4\,x\,(2M\log_2 M+2M)$<br>PPN: $8KM$ | 11264 | 24576 |
| DFT spreading | 1 DFT, 2 IFFTs and 2PPNs | DFT: $4\,x\,(M/2\log_2 M)$<br>IFFT: $4\,x\,(2M\log_2 M+2M)$<br>PPN: $8KM$ | 12032 | 26368 |
| Improved DFT | 1 DFT, 2 IFFTs and 2PPNs | | 12032 | 26368 |
| ITSM | 1 DFT, 2 IFFTs and 2PPNs | | 12032 | 26368 |
| Improved ITSM | 1 DFT, 2 IFFTs and 2PPNs | | 12032 | 26368 |
| GDFT spreading | 1 DFT, 1 GDFT,2 IFFTs and 2 PPNs | GDFT: $4\,x\,(M\ \log_2 M)$<br>DFT: $4\,x\,(M/2\log_2 M)$<br>IFFT: $4\,x\,(2M\log_2 M+2M)$<br>PPN: $8KM$ | 13568 | 19456 |
| Improved GDFT | 1 DFT, 1 GDFT,2 IFFTs and 2 PPNs | | 13568 | 19456 |

# 7. CONCLUSIONS

In FBMC, a higher PAPR is a major disadvantage. Using a single carrier effect is regarded as a useful strategy for reducing PAPR in FBMC systems with a minimal amount of complexity overhead. However, the FBMC PAPR reduction performance differs from the performance of the SC-FDMA technique. This is due to the overlapping structure of the OQAM FBMC symbols' in-phase and quadrature. In this paper, we proposed a novel algorithm for improving the PAPR performance of the single carrier techniques. The proposed algorithm was based on increasing the average power by increasing each FBMC symbol amplitude by utilizing a predetermined small value. we present a signal distortion-based algorithm for maintaining computational complexity while enhancing PAPR reduction performance in FBMC for single carrier effect techniques without the requirement for SI overhead. The presented technique is used in other FBMC single carrier effect algorithms. At various numbers of subcarriers, the PAPR performance of single carrier effect approaches is evaluated using the suggested methodology.

From the simulation results, the use of the proposed algorithm resulted in a major reduction of PAPR in the single carrier techniques namely, DFT, ITSM, and GDFT. This improvement in PAPR performance was achieved without any complexity overhead. In future work, other spreading techniques such as discrete cosine transform (DCT) and Hadamard transform should be investigated under the proposed algorithm.

## CONFLICTS OF INTEREST

The authors declare no conflict of interest.

## REFERENCES


[1] Liu, Y., Chen, X., Zhong, Z., Ai, B., Miao, D., Zhao, Z., Guan, H. Waveform Design for 5G Networks: Analysis and Comparison. *IEEE Access*, **5**, 19282–19292 (2017).

[2] Salem, M. A., Tarrad, I. F., Youssef, M. I., & El-kader, S. M. A. QoS Categories Activeness-Aware Adaptive EDCA Algorithm for Dense IoT Networks. *International Journal of Computer Networks & Communications*, **11(03)**, 67–83 (2019).

[3] Salem, M. A., Tarrad, I. F., Youssef, M. I., & El-kader, S. M. A. An Adaptive EDCA Selfishness-Aware Scheme for Dense WLANs in 5G Networks. IEEE Access, **8**, 47034–47046 (2020).

[4] Hussein, H. H., Elsayed, H. A., & Abd El-kader, S. M. Intensive Benchmarking of D2D communication over 5G cellular networks: prototype, integrated features, challenges, and main applications. *Wireless Networks*. **26**, 3183–3202 (2020).

[5] Le, L. B., Lau, V., Jorswieck, E., Dao, N.-D., Haghighat, A., Kim, D. I., & Le-Ngoc, T. Enabling 5G mobile wireless technologies. *EURASIP Journal on Wireless Communications and Networking*, **218**, (2015).

[6] Mitra, R. N., & Agrawal, D. P. 5G mobile technology: A survey. *ICT Express*, **1(3)**, 132–137 (2015).

[7] Gerzaguet, R., Bartzoudis, N., Baltar, L. G., Berg, V., Doré, J.-B., Kténas, D., Roth, K. The 5G candidate waveform race: a comparison of complexity and performance. *EURASIP Journal on Wireless Communications and Networking*, **13**, (2017).

[8] Hussein, H. H., & Abd El-Kader, S. M. Enhancing signal to noise interference ratio for device to device technology in 5G applying mode selection technique. *2017 Intl Conf on Advanced Control Circuits Systems (ACCS) Systems & 2017 Intl Conf on New Paradigms in Electronics & Information Technology (PEIT)*, (2017).

[9] Farhang-Boroujeny, B. Filter Bank Multicarrier Modulation: A Waveform Candidate for 5G and beyond. *Advances in Electrical Engineering*, **2014**, 1–25 (2014).

[10] Buzzi, S., Ugolini, A., Zappone, A., & Colavolpe, G. An Introduction to Modulations and Waveforms for 5G Networks. *Signal Processing for 5G*, 1–23 (2016).

[11] Schaich, F., & Wild, T. Waveform contenders for 5G - OFDM vs. FBMC vs. UFMC. *2014 6th International Symposium on Communications, Control and Signal Processing (ISCCSP)*, (2014).

[12] Dang, J., Zhang, Z., Wu, L., & Wu, Y. A New Framework of Filter Bank Multi-Carrier: Getting Rid of Subband Orthogonality. *IEEE Transactions on Communications*, **65(9)**, 3922–3932 (2017).
[13] Wang, H., Wang, X., Xu, L., & Du, W. Hybrid PAPR Reduction Scheme for FBMC/OQAM Systems Based on Multi Data Block PTS and TR Methods. *IEEE Access*, **4**, 4761–4768 (2016).
[14] Wang, H. A Hybrid PAPR Reduction Method Based on SLM and Multi-Data Block PTS for FBMC/OQAM Systems. *Information*, **9(10)**, 246 (2018).
[15] Nadal, J., Nour, C. A., & Baghdadi, A. Design and Evaluation of a Novel Short Prototype Filter for FBMC/OQAM Modulation. *IEEE Access*, **6**, 19610–19625 (2018).
[16] El-Basioni, B. M. M., Moustafa, A. I., El-Kader, S. M. A., & Konber, H. A. Timing Structure Mechanism of Wireless Sensor Network MAC layer for Monitoring Applications. *International Journal of Distributed Systems and Technologies*, **7(3)**, 1–20 (2016).
[17] Kobayashi, R. T., & Abrao, T. FBMC Prototype Filter Design via Convex Optimization. *IEEE Transactions on Vehicular Technology*, **68(1)**, 393–404 (2019).
[18] Yuen, C. H. (George), Amini, P., & Farhang-Boroujeny, B. Single carrier frequency division multiple access (SC-FDMA) for filter bank multicarrier communication systems. *Proceedings of the 5th International ICST Conference on Cognitive Radio Oriented Wireless Networks and Communications*, (2010).
[19] Ihalainen, T., Viholainen, A., Stitz, T. H., Renfors, M., & Bellanger, M. Filter bank based multi-mode multiple access schemes for wireless uplink. In *2009 17th European Signal Processing Conference*, 1354-1358 (2009).
[20] Na, D., & Choi, K. Low PAPR FBMC. *IEEE Transactions on Wireless Communications*, **17(1)**, 182–193 (2018).
[21] Aboul-Dahab, M. A., Fouad, M. M., & Roshdy, R. A. Generalized Discrete Fourier Transform for FBMC Peak to Average Power Ratio Reduction. *IEEE Access*, **7**, 81730–81740 (2019).
[22] R. P. Junior, C. A. F. d. Rocha, B. S. Chang and D. Le Ruyet, "A Generalized DFT Precoded Filter Bank System," in *IEEE Wireless Communications Letters*, vol. 11, no. 6, pp. 1176-1180, June 2022, doi: 10.1109/LWC.2022.3160301.
[23] M. Muthuramalingam and K. Venusamy, "Implementation of Pruned DFT Spread Filter Bank Multicarrier System for Low PAPR," *2022 6th International Conference on Trends in Electronics and Informatics (ICOEI)*, 2022, pp. 261-266, doi: 10.1109/ICOEI53556.2022.9777215.
[24] N. A. Mohamed Al Harthi, Z. Zhang and S. Choi, "FBMC-OQAM PAPR Reduction Schemes," *2020 International Conference on Information and Communication Technology Convergence (ICTC)*, 2020, pp. 148-150, doi: 10.1109/ICTC49870.2020.9289244.
[25] Kollár, Z., & Horváth, P. PAPR Reduction of FBMC by Clipping and Its Iterative Compensation. *Journal of Computer Networks and Communications*, **2012**, 1–11 (2012).
[26] Ihalainen, T., Ikhlef, A., Louveaux, J., & Renfors, M. Channel Equalization for Multi-Antenna FBMC/OQAM Receivers. *IEEE Transactions on Vehicular Technology*, **60(5)**, 2070–2085 (2011).
[27] Deng, H., Ren, S., Liu, Y., & Tang, C. Modified PTS-based PAPR Reduction for FBMC-OQAM Systems. *Journal of Physics: Conference Series*, **910**, (2017).
[28] Kollár, Z., & Horváth, P. PAPR Reduction of FBMC by Clipping and Its Iterative Compensation. *Journal of Computer Networks and Communications*, **2012**, 1–11 (2012).
[29] AboulDahab, M. A., Fouad, M. M., & Roshdy, R. A. A proposed preamble-based channel estimation method for FBMC in 5G wireless channels. *2018 35th National Radio Science Conference (NRSC)*, (2018).
[30] Roshdy, R. A., Aboul-Dahab, M. A., & Fouad, M. M. A Modified Interference Approximation Scheme for Improving Preamble Based Channel Estimation Performance in FBMC System. International Journal of Computer Networks & Communications, **12(1)**, 19–35(2020).
[31] Weiss, S. Efficient subband adaptive filtering with oversampled GDFT filter banks. *IEE Colloquium on Adaptive Signal Processing for Mobile Communication Systems*, (1997).
[32] Kollar, Z., & Al-Amaireh, H. FBMC Transmitters with Reduced Complexity. *Radioengineering*, **27(4)**, 1147–1154 (2018).
[33] Chin-Liang Wang, & Yuan Ouyang. Low-complexity selected mapping schemes for peak-to-average power ratio reduction in OFDM systems. *IEEE Transactions on Signal Processing*, **53(12)**, 4652–4660 (2005).
[34] Shrivastava, S., Jain, A., & Soni, R. K. Performance Analysis of FBMC System for Next Generation of Wireless Network. Journal of Advanced Research in Dynamical and Control Systems, **11 (11)**, 126–131(2019).